

LA-5616-PR

Progress Report

SPECIAL DISTRIBUTION

Issued: May 1974

**C. 3**

**CIC-14 REPORT COLLECTION  
REPRODUCTION  
COPY**

Quarterly Report

# Joint Services Explosives Program

December 1, 1973, through March 15, 1974

Compiled by

A. Popolato



**los alamos  
scientific laboratory**

of the University of California

LOS ALAMOS, NEW MEXICO 87544



This report was prepared as an account of work sponsored by the United States Government. Neither the United States nor the United States Atomic Energy Commission, nor any of their employees, nor any of their contractors, subcontractors, or their employees, makes any warranty, express or implied, or assumes any legal liability or responsibility for the accuracy, completeness or usefulness of any information, apparatus, product or process disclosed, or represents that its use would not infringe privately owned rights.

This series of reports presents the status of the LASL Joint Services Explosives Program. Other reports in this series, all unclassified, are:

LA-5402-PR

LA-5521-PR

In the interest of prompt distribution, this progress report was not edited by the Technical Information staff.

This work was performed with funds provided by the Defense Advanced Research Projects Agency under DARPA Order No. 2502.

## CONTENTS

I. SUMMARY REPORT	1
A. Physical and Processing Characteristics of Nonideal Explosives - Special Emphasis on Amatex (Task A)	1
B. Analysis of Prematures (Task B)	2
C. Synthesis of HMX (Task C)	3
D. Initiation and Sensitivity (Task D)	3
II. PROGRESS REPORT	3
A. Physical and Processing Characteristics of Nonideal Explosives - Special Emphasis on Amatex (Task A)	3
B. Analysis of Prematures (Task B)	15
C. Synthesis of HMX (Task C)	18
D. Initiation and Sensitivity (Task D)	18
REFERENCES	18
DISTRIBUTION	20

LOS ALAMOS NATL. LAB. LIBS.



3 9338 00377 1853

JOINT SERVICES EXPLOSIVES PROGRAM  
QUARTERLY PROGRESS REPORT  
FOR THE PERIOD DECEMBER 1, 1973 THROUGH MARCH 15, 1974

compiled by

A. Popolato

PREFACE

This is the third of a series of progress reports describing the status of four tasks undertaken by the Los Alamos Scientific Laboratory (LASL) for the Defense Advanced Research Projects Agency. The intent of LASL is to issue these reports on a quarterly basis. Since the tasks undertaken by LASL form an integral part of the Joint Services Explosive Program, copies of this report are being distributed to the agencies of the services participating in the program. Separate final reports will be issued for each of the tasks at the termination of each task.

ABSTRACT

The results obtained, for the period from December 1, 1973 through March 15, 1974, on the Joint Services Explosive Program are presented. The tasks undertaken by the Los Alamos Scientific Laboratory include: (1) Physical and Processing Characteristics of Nonideal Explosives - Special Emphasis on Amatex, (2) Analysis of Prematures, (3) Synthesis of HMX, and (4) Initiation and Sensitivity.

---

I. SUMMARY REPORT

A. PHYSICAL AND PROCESSING CHARACTERISTICS OF NONIDEAL EXPLOSIVES - SPECIAL EMPHASIS ON AMATEX (TASK A)

1. Introduction

During the past quarter, emphasis has been placed on the processing aspects of Amatex (mixtures of RDX, TNT, and ammonium nitrate (AN)), in particular, the preparation of melts and casting of charges. The results of earlier work, funded by Picatinny Arsenal (PA), indicated that the flow properties of Amatex/20 melts were dependent upon the particle size distribution of the AN used to prepare the melt.

Variations in melt viscosity are undesirable in ammunition loading operations. A method of reducing viscosity variability is to impose rigid requirements on the AN granulation. This approach is expensive. Another, less expensive, method is to add surface active agents to reduce variations in viscosity due to changes in particle size. For this reason, work with surface active agents was undertaken.

The irreversible growth of Amatex formulations caused by the solid-solid phase transitions in AN pose a serious storage problem. This problem can be solved by the addition of potassium nitrate (KN). The ideal solution would be to prevent a

phase change over the temperature range of military interest. Work on the phase diagram of the AN-KN system was undertaken to aid in solving this problem.

Preliminary studies on the shock initiation properties of Amatex formulations have been started.

## 2. Progress This Report Period

### a. Amatex Processing Study

Two surface active compounds, nitrocellulose (NC) and decyl gallophenone (DGP), have been found to reduce the apparent viscosity of Amatex melts. With the addition of 0.10 wt% NC or 0.05 wt% DGP, the apparent viscosity of an Amatex melt composed of 20 wt% RDX/45 wt% granulated AN/35 wt% TNT was reduced by a factor of 10 under conditions of constant shear stress, and the yield value or the stress required to produce flow was reduced by a factor of 3. Other surface active compounds were tried without success.

The addition of 0.05 wt% NC to Amatex melts prepared with AN prills resulted in a homogeneous dispersion of prills both in the melt and in the casting. The effect of the NC is to reduce the interfacial tension between the AN and the TNT. This finding is significant because it makes possible the preparation of melts without the use of vacuum, since the prills do not segregate to the riser during the casting operation. The use of fertilizer grade prills, without a requirement for grinding, could significantly reduce the manufacturing costs of Amatex. If there is no change in either energy or initiability with AN particle size, then there is no real requirement for grinding.

### b. The AN-KN Phase Diagram

Work on the AN-KN phase diagram over a temperature range of -50 to 170°C and a composition range of 0 to 30 wt% KN has been completed. Results of this work indicate that there is no thermodynamically stable phase in this range of

composition between -50 and 85°C. With AN containing 16 to 18 wt% KN, a single thermodynamically stable phase exists between -15 and 110°C. At temperatures below -20°C, the slow kinetics associated with the phase transition could result in a kinetic stability.

## 3. Future Work

Work with NC will be continued to determine the optimum concentration. The relative energy of Amatex formulations as a function of particle size, including prills, will be determined. Preliminary studies on the initiation properties of Amatex as a function of AN particle size should be nearing completion by the end of the next quarter.

## B. ANALYSIS OF PREMATURES (TASK B)

### 1. Introduction

Although a wide variety of projectile defects have been suggested as possible causes of prematures, this study considers only the effects of defects in the explosive and of the type of explosive fill.

The objective of this study is to develop a number of analytical models that simulate the ways in which thermal energy is generated and transported into the explosive. The generation of thermal energy will be calculated as a function of the type of defects in the explosive, the type of explosive, and the force fields experienced by the explosive in the gun tube. The ultimate goal is to identify the critical parameters leading to initiation and then to verify these parameters experimentally.

### 2. Progress This Report Period

The closure of a base gap by the setback forces, imparted to the projectile during its acceleration through the gun tube, was simulated experimentally with an "aquarium" test. Although the rate of gap closure did not duplicate the rate experienced in an artillery projectile, the basic mechanism of generating thermal energy through the compression of a gas in the void and its transport into the surroundings was duplicated. In a

parallel analytical study, one-dimensional calculations were made with a reactive hydrodynamic code, SIN, to simulate the gap closure. The hydrodynamic state values at maximum compression were used as the initial conditions in a reactive heat conduction calculation to determine the extent of reaction in the high explosive.

Experimentally, decomposition, or evidence of burn, was observed with separations of 1 mm and the degree of decomposition was independent of the type of gas in the void (air, krypton, methane, or vacuum). However, our calculations show that, with a 1-mm air gap closed in  $6.5 \mu\text{s}$ , and a gas temperature of 2700 K, insufficient reaction occurred to cause the first HE (TNT) cell to decompose. As time progressed, the explosive surface cooled, since heat was being conducted away faster than it was being furnished by hot gases and generated by the explosive decomposition.

The discrepancy between the calculation and the experiment indicates that some mechanism other than plane surface heat conduction is dominating the initiation process in the aquarium experiment when gaps of about 1-mm thickness are present.

### 3. Future Work

Additional aquarium tests will be performed with explosives having "defect free" surfaces. Polishing techniques are being developed in an effort to prepare these surfaces. Other initiation models, utilizing internal surface defects, and methods of concentrating energy in the defects will be tried to determine if sufficient thermal energy is generated to initiate ignition.

### C. SYNTHESIS OF HMX (TASK C)

Funds allocated to this task were expended during the first two quarters, and results were reported in the two quarterly reports previously issued.

Additional work is being conducted with funds provided by PA.

### D. INITIATION AND SENSITIVITY (TASK D)

#### 1. Introduction

The ultimate objective of this investigation is to obtain a quantitative understanding of the mechanisms leading to the initiation of a violent reaction in the high explosive. One approach to developing a quantitative model of the initiation is to study the response of an explosive subjected to a single shock of known amplitude and duration in a one-dimensional system. This requires the development of a plane wave shock generator and supporting instrumentation for experiments that will generate data that can be used to determine the state of the shocked explosive as a function of time and initial conditions.

#### 2. Progress This Report Period

Considerable difficulty has been encountered in the design of a flyer plate, plane wave shock generator. A study of the response of explosives cannot be started until these problems have been resolved.

#### 3. Future Work

Work will continue on the design of plane wave generators and the instrumentation required to measure the amplitude and duration of the shock pulse.

## II. PROGRESS REPORT

### A. PHYSICAL AND PROCESSING CHARACTERISTICS OF NONIDEAL EXPLOSIVES - SPECIAL EMPHASIS ON AMATEX (TASK A), A. Popolato, T. Rivera, H. H. Cady

#### 1. Introduction

During the past quarter, emphasis has been placed on processing related to the preparation and casting of Amatex, mixtures of RDX, TNT, and AN. The results of earlier work<sup>1</sup> funded by PA indicated that the viscosity of the Amatex slurry and the properties of the cast Amatex were, as expected, related to the particle size distribution of the AN used to prepare the material.

Variations in viscosity are undesirable in ammunition loading operations. If the major

source of variations in viscosity is the variation in AN granulation, one method of reducing the variability is to impose a control on the AN grinding operation. This method of viscosity control is expensive. Another, less expensive method is to use surface active compounds that tend to reduce differences in viscosity due to variations in AN granulations. For the AmateX system, the surface active compound should reduce the interfacial tension between the solid AN phase and the liquid TNT.

Work relating to the phase stabilization of AN with KN has continued and is nearing completion.

Preliminary studies related to shock initiation characteristics of AmateX have been started. The results of this study are important to the munition design in that they should provide the information required to design a reliable boosting and fusing system.

## 2. Progress This Report Period

### a. Preliminary Studies with Surface Active Compounds

The purpose of these studies was to find a surface active compound that would improve the flow properties of AmateX melts containing ground AN.

The choice of wetting agents was based on previous experience with castable TNT systems and on a review of manufacturers' literature describing surface active compounds. NC, DGP, and steroxy acetic acid (SAA), are routinely used to improve the flow properties of Baratols (barium-nitrate-TNT systems) and Boracitols (boric acid-TNT systems).

A list of the surface active chemicals tried with AmateX/20 and a qualitative evaluation of the wetting properties is shown in Table I. The preliminary evaluation and screening was made by visual and microscopic observation. Small melts (~4 g) consisting of 10 wt% AN prills\*/90 wt% TNT/0.1 wt% surface active compound were prepared.

\*AN prills meeting the requirements specified in MIL-A-50460 procured from Terra Chemicals International, Inc., Sioux City, Iowa, were used.

TABLE I  
AMATEX SURFACE ACTIVE COMPOUNDS  
SCREENING TESTS<sup>a</sup>

Surface Active Compound	Source	Qualitative Results
None	-	Poor wetting, AN prills unfilled
NC (18-25 cps, 11.8-12.2% N)	Hercules Chemical	Good wetting, AN prills unfilled
DGP	LASL-synthesized	Good wetting, AN prills filled
SAA	DuPont	Fair wetting, AN prills unfilled
Aerosol OT	American Cyanamid	Good wetting, AN prills filled
Versamid 125	General Mills	Did not dissolve in TNT
Terigitol NPX	Union Carbide, Carbon Chemical	Incompatible - TNT turned red
Triton X114	Rohm and Haas	Incompatible - TNT turned red
Triton X100	"	Incompatible - TNT turned red
VM 5336	DuPont	Good wetting, AN prills filled
Oleic acid		Good wetting, AN prills filled
Duponol	DuPont	Did not dissolve in TNT
Methocel NF	Dow Chemical	Poor wetting, AN prills not filled
Span 60	Atlas Powder	Poor wetting, AN prills not filled
Fluorocarbon FC-95	Minnesota Mining & Mfg.	Poor wetting, AN prills not filled

<sup>a</sup>0.1% surface active agent used in a mixture of 90 wt% TNT/10 wt% AN prills.

The melts were observed with the aid of a microscope to determine the degree of wetting. Visual observation of the flow of TNT into the prill cavity was considered evidence of wetting. A change in color was considered preliminary evidence of chemical incompatibility. Seven of the compounds tried were selected for further study. Melts containing one-third each AN/RDX/TNT, by weight plus

0.2 wt% surface active compound were prepared and the thermal stability of the mixtures was determined. The results obtained in thermal vacuum stability, pyrolysis, and differential thermal analysis (DTA) tests are presented in Table II. The results of these tests led to the choice of NC, SAA, DGP, and Aerosol OT for further study.

TABLE II  
COMPATIBILITY SCREENING TESTS

Surface Active Agent	Vacuum Stability (ml/g, 120°C 48 h)	DTA (°C) No Significant Exotherm Below	Pyrolysis (°C) No Significant Gas Evolved Below
None	1.9	190	160
DGP	4.8	"	"
NC	2.2	"	"
SAA	2.1	"	170
4-Capryl resorcinol	5.8	"	"
Aerosol OT	2.1	"	"
VM 5336	9.0	"	"
Oleic acid	8.5	"	"

(1) Viscometer Calibration. A Stormer viscometer<sup>2</sup> was used to determine the effect of surface active compounds on the flow properties of Amatex. The Stormer or rotational viscometer was chosen because a more quantitative evaluation of the flow on non-Newtonian systems could be obtained.

Because of the tendencies of the solid phases, RDX and AN, to segregate, the Stormer was modified by replacing the cylindrical rotating member with a two-bladed rotating impeller. Before use, the modified viscometer was calibrated with a Newtonian fluid over a viscosity range of 10 to 37 P. Castor oil was used as the calibrating fluid and the viscosity was varied by changing the temperature of the fluid.

For a rotational viscometer driven by a falling weight, the viscosity,  $\eta$ , can be expressed as a function of the weight,  $W$ , and the rotational speed of the impeller,  $\Omega$ , as follows:

$$\eta = K \frac{(W - W_0)}{\Omega} \quad (1)$$

where

$K$  = A characteristic constant related to the geometry of the impeller, size of the stationary member, etc.

$W_0$  = The frictional resistance of the viscometer in grams

$\Omega$  = The rotational speed of the impeller in revolutions per second

The derivation of this expression assumes Newtonian flow.<sup>3</sup> For non-Newtonian flow, the coefficient of viscosity is not a constant. The flow properties of these materials are characterized in terms of an apparent viscosity at a specified rate of shear (impeller speed) or shear stress (weight), with or without a given yield value (shear stress required to initiate flow).

The results of the Stormer viscometer calibration are presented in Fig. 1. Linearity indicates that the calibration fluid is Newtonian.

(2) Effect of Surface Active Agents on Flow Properties of Amatex. The Amatex melts used in this study were prepared with Composition B meeting the requirements specified in MIL-C-401C for Grade A Comp. B; AN meeting the requirements specified in MIL-A-50460, Amendment 1; and TNT meeting the requirements specified in JAN-T-248 for Grade 1 TNT. The particle size distribution of the RDX in the Comp. B is shown in Fig. 2. Both prilled (as received) and granulated AN were used. The granular material was prepared by grinding the prills in a Model 5H Mikro



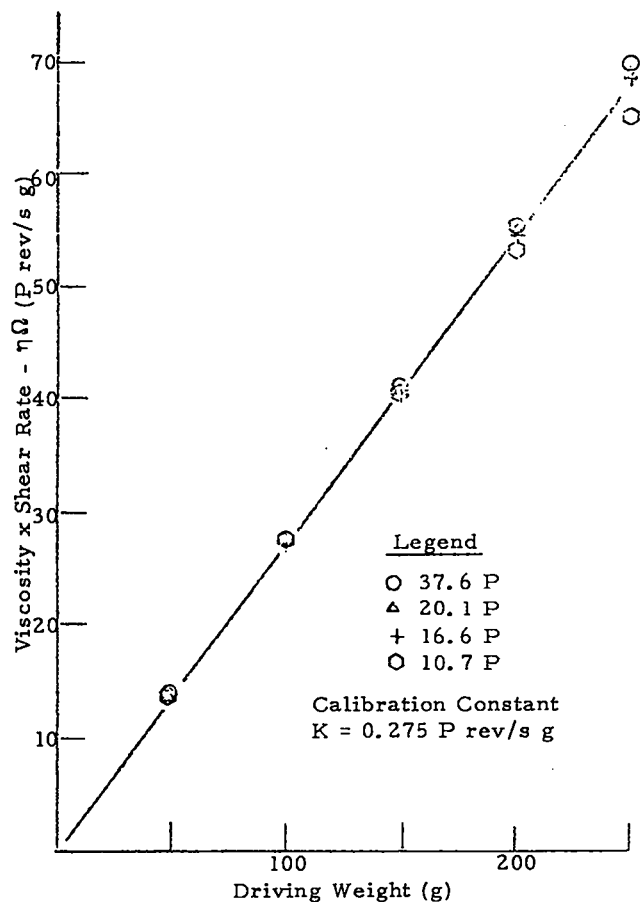


Fig. 1. Modified Stormer viscometer calibration.

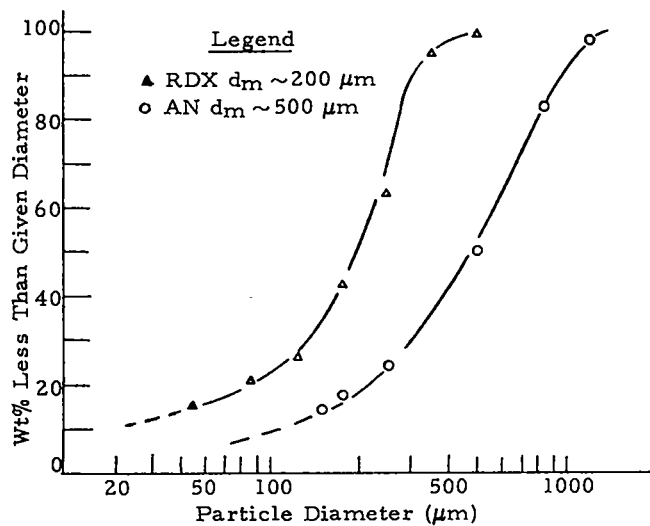


Fig. 2. Particle size distribution of RDX and AN.

Pulverizer hammer mill to the particle size distribution shown in Fig. 2.

The flow properties of Amatex/20 melts prepared with granulated AN, prilled AN, and granulated AN containing 0.05% NC\* are shown graphically in Fig. 3. and are tabulated in Table III.

\*The nitrogen content of the NC used in this study was 11.8-12.2% and the viscosity was 18-25 cP.

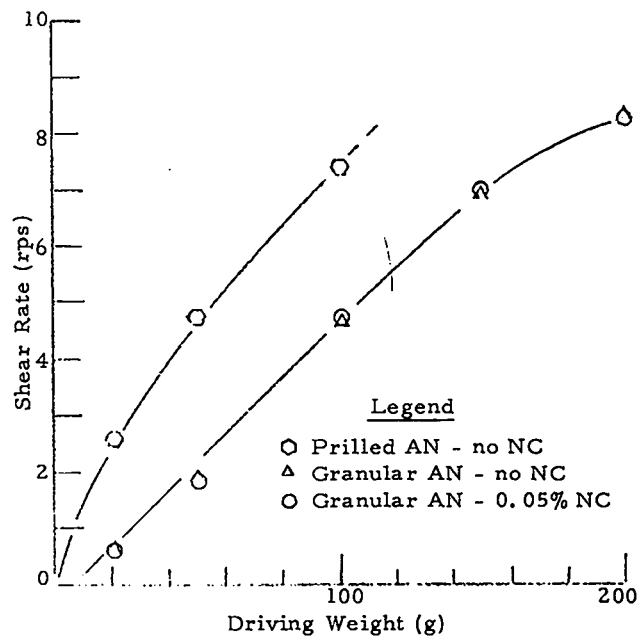


Fig. 3. Flow Properties of Amatex/20.

TABLE III  
FLOW PROPERTIES OF AMATEX/20<sup>a</sup>

AN Particle Size	Surface Active Agent (%)	Yield Value (g)	Apparent Viscosity (P) Stormer at Constant Shear		
			Rate 2 rps	Stress 200 g	Efflux (s)
Prills	0	0	2.5	-	3
Ground <sup>b</sup>	0	10	6.9	5.8	12
Ground <sup>b</sup>	0.05	10	6.9	5.8	-

<sup>a</sup>The RDX particle size distribution is shown in Fig. 2.

<sup>b</sup>The AN particle size distribution is shown in Fig. 2.

Analyses of the data shown in Fig. 3 and Table III indicate that Amatex/20 prepared with either AN prills or with granulated AN is quite fluid and offers no casting problems. There is no significant change in the flow properties due to the addition of NC.

So that the effects of the surface active compounds could be more easily observed, in a less fluid melt, the quantity of TNT was reduced from 40 to 35 wt% and the quantity of AN was increased to 45 wt%. The effects of surface active compounds on this mixture, called Amatex/20-45, are shown in Table IV and Fig. 4. Results of this experiment indicated that both NC and DGP improved the flow properties of Amatex. With either 0.1 wt% NC or 0.05 wt% DGP, the yield value was decreased by a factor of 3 and the apparent viscosity, at a constant shear stress of 200 g, by a factor of 10. The melts containing 0.1 wt% NC and 0.05 wt% DGP were castable. Casting problems were encountered with the remaining melts.

TABLE IV  
EFFECT OF SURFACE ACTIVE AGENTS  
ON FLOW PROPERTIES OF AMATEX<sup>a</sup>  
(20 wt% RDX/45 wt% AN/35 wt% TNT)  
Temperature - 84°C

Surface Active Agent	Amount (wt%)	Yield Value (g)	Apparent Viscosity (P) at Constant Shear	
			Rate 2 rps	Stress 200 g
None	0	180	50	220
NC	0.05	130	37	55
NC	0.10	60	24	22
SAA	0.05	180	50	220
DGP	0.05	60	24	22
Aerosol OT	0.05	200	52	∞

<sup>a</sup>The particle size distribution of the RDX and AN used is shown in Fig. 2.

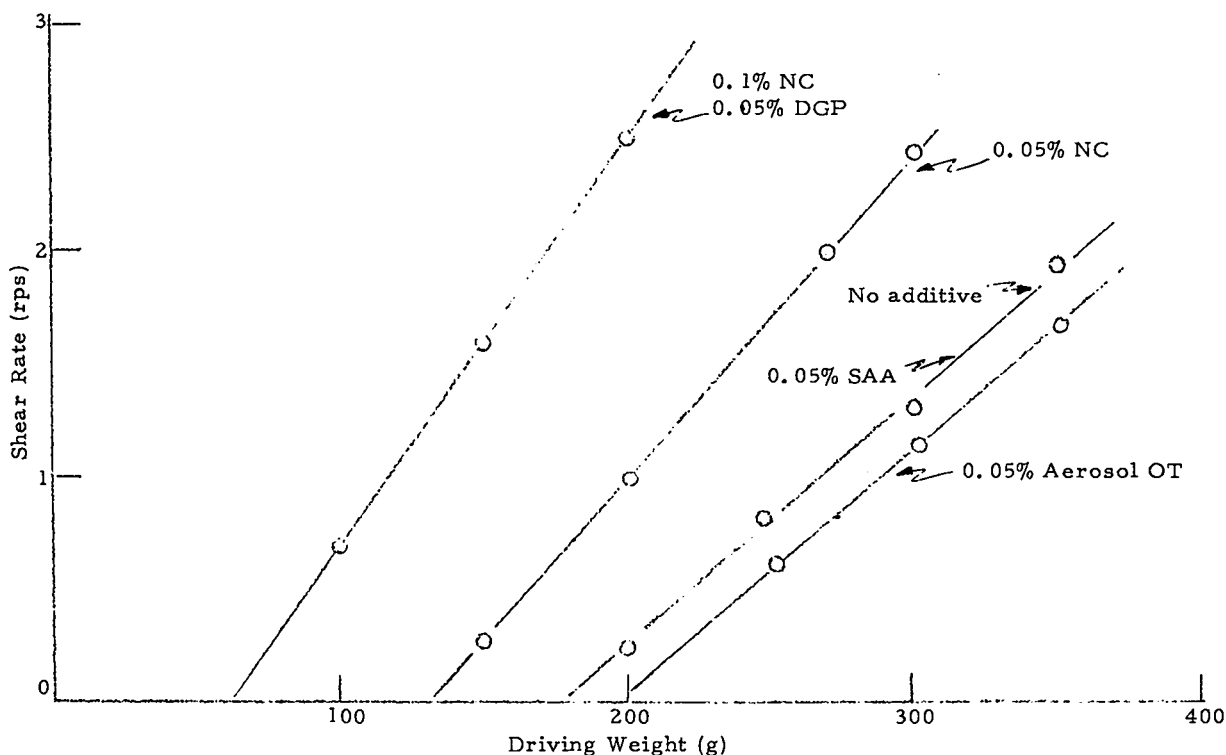


Fig. 4. Flow Properties of Amatex (20 wt% RDX/45 wt% AN/35 wt% TNT)

Since there was no apparent difference between NC and DGP, work with DGP was discontinued because NC is readily available and inexpensive.

The effect of total solids content on the viscosity of a series of Amatex melts made with prills is shown in Table V and Fig. 5. The most important finding of this study is that the AN prills, in Amatex containing NC, do not segregate. During

the casting operation, there was no evidence of prill segregation into the riser portion of the casting. This finding could be important in a production operation since it could lead to the preparation of homogeneous Amatex castings made with prills without resorting to the use of vacuum.

Another important result is that with prills, the TNT content can be reduced to 35 wt% and the AN increased to 45 wt% without making significant changes in the casting properties.

(3) Preparation of Fine (1-20  $\mu$ m) AN. A study of the effect of AN particle size on the performance of Amatex has been conducted with AN particles whose size ranged from 50 to 500  $\mu$ m and no significant effect has been found.

Results of calculations<sup>4</sup> indicate that over this range of particle size, half the AN acts as if it is unreacted when the Amatex is fired. If we can show that the degree of reaction cannot be increased, even with the finest AN particles available, and that the initiation properties are also independent of particle size, then requirements for granulation can be relaxed.

Because of the hygroscopic properties of granular AN, a coprecipitation procedure was used to prepare the AN. A solution containing 100 g of TNT in 500 ml of toluene was cooled to about 3°C. Another solution containing 100 g of AN in 500 ml of methanol was heated to about 55°C. The AN-methanol solution was poured into the TNT-toluene solution, and the precipitate obtained was filtered, washed with about one liter of n-octane, and dried under vacuum at 50°C for about 12 h. The dried precipitate contained some large agglomerates of material that were removed by screening with a 20-mesh screen. A sample of the remaining powder was placed on a microscope hot stage that was heated to the melting point of TNT and observed under polarized light. The results of the observations indicated that the AN particles were coated with a layer of TNT. This coating gives the AN particles some water-repellant characteristics.

TABLE V  
VISCOSITY OF AMATEX MADE WITH  
PRILLED AN  
Temperature - 84°C

Composition (wt%)				Yield Value (g)	Apparent Viscosity (P) at Constant Shear	
RDX	AN	TNT	NC		Rate 2 rps	Stress 200 g
40	20	40	0	0	2.5	5.6
20	40	40	0	0	2.7	6.0
20	45	35	0.05	0	3.8	6.3
20	50	30	0.05	50	11.0	14.0

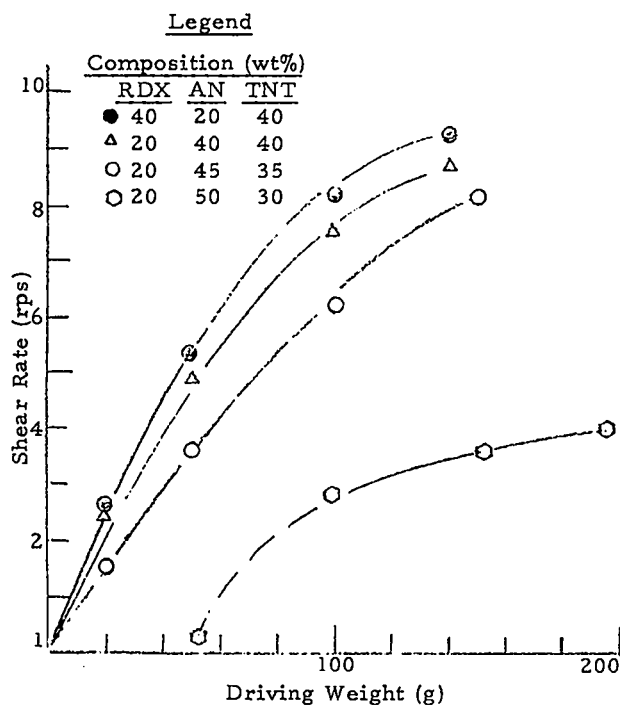


Fig. 5. Flow properties of Amatex made with prilled AN.

The AN particle size distribution appeared to lie within a 10- to 100- $\mu$ m range. Further efforts will be made to obtain a particle size distribution lying within the 1- to 20- $\mu$ m range.

b. The AN-KN Phase Diagram

(1) Introduction. The Naval Ordnance Laboratory (NOL) reported<sup>5</sup> that the addition of  $\text{KNO}_3$  (KN) in solid solution to the AN used in Minol improved the dimensional stability of the Minol charges. The mechanism proposed for this increased stability was that KN prevented the transformation of AN III to AN IV (the normally stable form) in the temperature range studied. The discrepancies in the literature concerning the AN-KN phase diagram and the confusion between kinetics of the AN polymorphic transformations, and the thermodynamics of these transformations, require a redetermination of the phase diagram in order to provide the information necessary to select the optimum AN-KN composition to meet military storage conditions.

The last quarterly report<sup>4</sup> listed many of the literature reports pertinent to this study and summarized the preliminary experiments. In this report, we give the results for the study in the AN rich end of the system up to 30 wt% KN. This is the portion of the system of most interest with respect to its use in Amatex, and is also the region in which we have concentrated our efforts to determine the true phase diagram.

(2) Experimental Program. Slow reactions, especially the transformations involving AN III, create a problem in determining the phase diagram of the system. Water catalyzes the AN III-AN IV transformation.<sup>5</sup> Pure water is also a very good solvent, especially for AN, and it is difficult to add an amount insufficient to dissolve an appreciable fraction of the small samples examined and perhaps alter the equilibrium composition of the solid phases remaining. Small amounts of ethylene glycol, or ethylene glycol with a few volume percentages of water, are nearly as effective catalysts

as water but do not dissolve significant portions of the samples. Ethylene glycol boils at a higher temperature than water and dilute solutions with water freeze at a lower temperature, thus increasing the temperature range available for the catalyst. Where practical, microscopic DTA and x-ray experiments were carried out in duplicate with one set of samples dry and another dampened with ethylene glycol. Results were compared carefully to ensure that ethylene glycol was acting only as a catalyst and did not in fact react, thereby altering the thermodynamics of the phases studied. Ethylene glycol is miscible with AN-rich melts which means that measurements involving a liquid phase, such as at the eutectic melting temperatures, are slightly lower with "wet" than dry samples and these wet sample values were ignored.

Brown and McLaren reported<sup>6</sup> that the transition sequence, AN V  $\rightarrow$  AN IV  $\rightarrow$  AN II  $\rightarrow$  AN I, proceeds with minor molecular reorientations as a sequence of solid-solid transformations while the transformations involving AN III are reconstructive. The catalysis of the AN III transformations by water or ethylene glycol confirms this hypothesis and explains why it was easier to study transformations involving AN III wet, while the other transformations could be observed equally well dry. This means that the metastable phase transitions between AN IV and AN II were measured dry while the metastable transitions between AN III and AN V were measured wet.

Fusion slides<sup>7</sup> covering the entire composition range in the AN-KN system were studied microscopically, and time-lapse photographs were taken over the temperature range from -55 to 165°C. The slides were easier to prepare if the slide and cover slip were treated with molten KN and then washed with distilled water. This treatment helps molten AN wet the glass and thus flow between the cover slip and slide into contact with the solid KN in the final stage of the fusion slide preparation. Fusion slides to be studied wet were touched with a wick wet with

ethylene glycol at the AN-KN junction until liquid could be seen to be drawn into the cracks in the salts. The cover slip was then sealed into position with quick setting epoxy. The epoxy functions to prevent the loss of solvent and sublimation of AN when the slide is held for prolonged times at high temperatures.

Observations of these fusion slides as a function of temperature were used to confirm the temperature stability ranges of the five polymorphs of AN and the stabilization of AN III, with respect to AN IV and AN II, by KN in solid solution. A material is observed in the intermediate region between pure AN and pure KN. This material has an increasing zone of stability as the temperature is increased to 126°C but eventually transforms to a phase isomorphous with KN I. This material does not have all the characteristics of a true compound but we will refer to its polymorphs as C I and C II in the present discussion. The rate of transformation of AN III to either AN IV or AN V decreases as the KN concentration increases. Wet fusion slides are ideal for transformation studies since they provide both adjacent seed crystals and a catalyst for the transformations. Even under these conditions detectable AN III remains after two weeks of cycling the sample between -20 and -60°C. However, the regions with less than 30% KN have transformed.

Mixtures of AN and KN for quantitative determinations of the phase boundaries were prepared by two techniques. Mixtures containing up to 30 wt% KN were formed by melting AN, dissolving KN in the melt, and rapid quenching by pouring the melt onto a sheet of Teflon. A limiting value of 30% KN was chosen because the temperature required to dissolve KN is increasing rapidly at the 30% KN concentration level and has reached the point at which AN is decomposing and/or vaporizing at a significant rate.

Jänecke, Hamacher, and Rahlfs<sup>6</sup> showed that the composition of the solid crystallized from solutions

at about 90°C is very nearly that of the solution. This fact was utilized in the second preparation technique in which solutions were evaporated to dryness at 90°C.

Hot and cold stage optical microscopy assisted by time-lapse photography was the most useful tool for determining the equilibrium transformation temperatures of the AN-KN mixtures. Typical sample preparation was accomplished in the following manner:

- A small crystal of KN was melted on a slide and crystallized by cooling.
- A portion of the mixture to be studied was placed on the slide, heated to melt the mixture, and covered quickly with a cover slip. Pressure, applied with a needle, was used to reduce the thickness of the mixture and to slide the cover slip until it was adjacent to the KN droplet so that the mixture could partially dissolve the pure KN.
- The slide was cooled quickly to recrystallize the mixture and then warmed in a narrow zone, at the opposite end of the cover slip from the KN, to a temperature sufficient to melt the pure AN that had been placed in contact with the edge of the cover slip.
- The sample was cooled to room temperature, treated with ethylene glycol, if desired, and potted with epoxy to complete the sample preparation.

This sample preparation technique generates the same complete spread in composition from pure AN to pure KN, as a fusion slide, but produces a wide band of known composition under the cover slip. Examination of the preparation near the pure AN or pure KN region was usually sufficient to indicate the position of the mixture with respect to the fusion slides.

Microscope hot stage (Mettler Model FP-2) temperature measurements could be made easily within  $\pm 0.3^\circ\text{C}$ ; however, subjective errors in

determining the stable phase usually cover a larger span in temperature so no effort has been made to correct the indicated temperatures. The microscope cold stage (Industrial Instruments Model CY3-A Thermoelectric Microscope cold stage) was a greater problem since the sample is cooled on only one side. Calibration of the stage showed that the temperature gradient across the field of view was often 1°C and subambient temperatures are probably accurate to no better than ±1°C. Temperatures were recorded as indicated by the sensing thermistor even when it was known that various portions of the sample were at different temperatures. The typical evidence for temperature or chemical gradients was the observation, in a given field of view, that a phase transition was proceeding in a direction in one portion of the viewing area and in the opposite direction in a different area.

A DuPont Model 900 differential thermal analyzer was used to study the rapid transitions in the system. Typical heating and cooling rates were 5°C/min. Wet samples were prepared by placing about 0.0005 cm<sup>3</sup> of ethylene glycol in the sample capillary, with a hypodermic syringe, before adding the sample. Measured transition temperatures agreed with those observed visually in the portion of the diagram reported here. Wet samples usually gave sharper, narrower, and less complex peaks than those obtained with dry samples.

A simple resistance-heated fused-quartz hot stage was constructed for the x-ray diffractometer. The surface temperature of the quartz was uniform within ±1°C and could be held at a known temperature or programmed in temperature as a function of time. This hot stage was useful above room temperature for studying dry samples that had been dusted onto the quartz surface. This hot stage had limited utility above 150°C because of the relatively rapid sublimation of AN in this temperature region and the corresponding change in sample composition.

An Enraf Nonius Model FR 524K low temperature device has been modified to provide a controlled temperature (-100 to 165°C) environment for an x-ray precession camera. The camera was modified to provide for sample rotation independently of the normal precession motion. These modifications turn the precession camera into a flat plate forward reflection powder camera limited to about 50° in 2θ. This camera has the advantage of a wider temperature range and samples are less subject to sublimation because they are held in sealed capillaries. This camera is being used to determine the species in equilibrium below -20°C.

(3) Phase Diagram. The phase diagram, as generated from the experimental data we have obtained, is given in Fig. 6. Data points were obtained by initiating a phase change and then

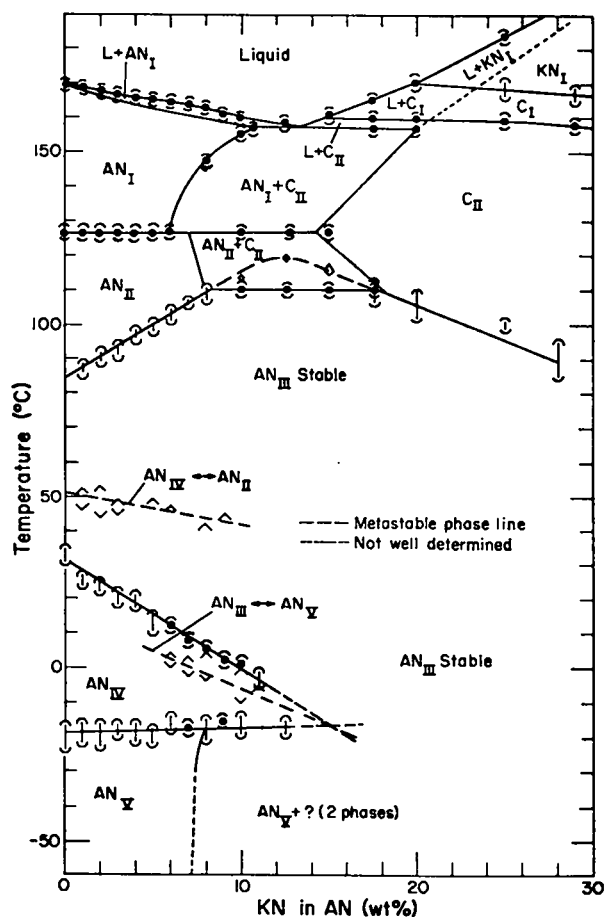


Fig. 6. AN-KN phase diagram (this investigation).

adjusting the temperature back and forth in decreasing increments, homing in on the equilibrium phase transition temperature. An essential part of the technique is the retention of both phases within the field of view during the entire experiment. Time-lapse photographs were used to determine the direction of crystal front growth and hence the stable phase for very slow reactions or reactions when temperatures were close to the equilibrium temperature. The lengths of the data point bars, Fig. 6, do not have their normal meaning but instead, represent the indicated temperature span between an observation in which the lower temperature phase was clearly stable to the indicated temperature at which the higher temperature phase was clearly stable. Single-ended data point bars mean that the transformation was observed in only one direction.

Phase boundaries between stable phases have been indicated by solid lines where their positions are known and by the dotted lines where their positions could only be inferred by extrapolation. Dashed lines are used to indicate boundaries between metastable phases.

The transformation rate of AN IV to AN V becomes slower as the KN concentration in the AN IV increases. The equilibrium-transformation line has a slight but definite positive slope with respect to KN. When the KN concentration in the initial AN IV is greater than 7 wt%, the AN V formed always shows the presence of an additional phase indicating a solubility limit of about 8% KN in AN V.

The metastable transformations between AN III and AN V are easy to observe in wet preparations containing 6 to 8% KN. This is true because this transformation is much faster than either AN III-AN IV or AN IV-AN V. The AN III-AN V transformation rate is very dependent on KN concentration and becomes nearly indistinguishable from the others when the KN concentration is greater than 9 wt%. AN V formed from AN III disproportionates

when the KN concentration exceeds 9%. The position of this phase line is reasonably well determined since it must cross the AN III-AN IV and AN IV-AN V phase lines where they intersect.

The position of the AN III-AN IV phase line has historically been the one that generated the most discussion. The results of this study indicate that many of the earlier studies were measuring kinetics and were not concerned with ensuring that the reactions were reversible. We find that solvents increase the rates of the AN III-AN IV transitions and greatly ease the determination of the equilibrium temperature. A solvent is not the only requirement for rapid transformations because we have also noticed that sample history affects the transformation. A typical example would be slides prepared by fusing pure AN. If the cover slip is in position when the sample melts in the initial slide preparation, then most of the water present in the original stock AN remains in the AN under the cover slip. The AN IV-AN III transformation can then be easily observed. However, if the AN IV is cooled to  $-50^{\circ}\text{C}$  before trying to measure the AN IV-AN III transformation, then initiating the AN III phase is difficult and the sample can be heated to the AN IV-AN II transition temperature. Frequently, the AN II formed will quickly transform to AN III. The AN III transforms to AN IV on cooling. Further cycles into the AN III region behave normally in that AN III seeds are present. Apparently, the transformation to AN V destroys nearly all AN III seed crystals. Precooled samples provided one technique for studying the AN IV-AN II transition. Another technique was to cool samples rapidly from the AN I phase region through AN II until they start transforming to AN IV. Often the phase change initiated the formation of stable AN III and insufficient time was available to reverse the metastable reaction before the sample had completely transformed to the stable phase. Many investigators report that the metastable AN IV-AN II phase line increases in temperature as the KN

concentration rises. This is most unlikely since the extrapolation of this phase line must also intersect the AN III-AN IV and AN III-AN II phase lines where they cross in the physically unattainable negative KN concentration region. The initial AN IV-AN II point is well determined and implies a decreasing temperature with increasing KN concentration.

The AN III-AN II phase line is relatively well behaved and easy to follow up to a 10% KN concentration. At higher KN concentrations two different paths can be observed. Under conditions of fast heating rates, AN III transforms reversibly to either AN III or C II depending on the particular KN concentration. Under slow heating conditions the AN II or C II formed often disproportionates into a mixture of these phases. Once these two phases are in intimate mixture, the equilibrium transformation temperature drops to 110°C for the three-phase AN III, AN II, C II transition.

AN II and C II are birefringent while AN I is isotropic so that it is easy to tell whether a portion of a mixture is undergoing transformation between AN I and AN II. This transition was used to determine the points of intersection with end points of the AN II-AN I phase line.

The position of the AN I and AN I + C II phase boundary is determined by appearance or disappearance of the birefringent phase. The top boundary of the AN I + C II region is determined by evidence of eutectic melting. Samples with 15% KN or more show a phase transition at 159 to 160°C. This transition occurs as a solid solid transition in samples with little or no melt. Another transition occurs about 10°C higher. The product of this second transformation is isomorphous with KN I. DTA curves show these two transformations as a double wave endotherm on heating; however, this reduces to a single wave as the KN concentration increases and hence the nomenclature C I for this high temperature phase. We have not been able to obtain an x-ray diffraction pattern for pure C I yet.

The AN III-C II phase boundary is difficult to determine precisely because reactions are slow and the two phases have a similar appearance under the microscope.

(4) Comparison with Literature. Jänecke et al.<sup>8</sup> published the first comprehensive phase diagram (Fig. 7) of the AN-KN system. Our results agree reasonably well with theirs in the 0 to 30% KN region. The most significant difference is in the AN III-AN IV phase boundary. Jänecke found a miscibility gap working in aqueous solutions while we did not find evidence of such a gap working in the solid state. A similar difference occurs between C II and AN III, although our visual evidence is insufficient to preclude such a gap. Jänecke missed the formation of C I.

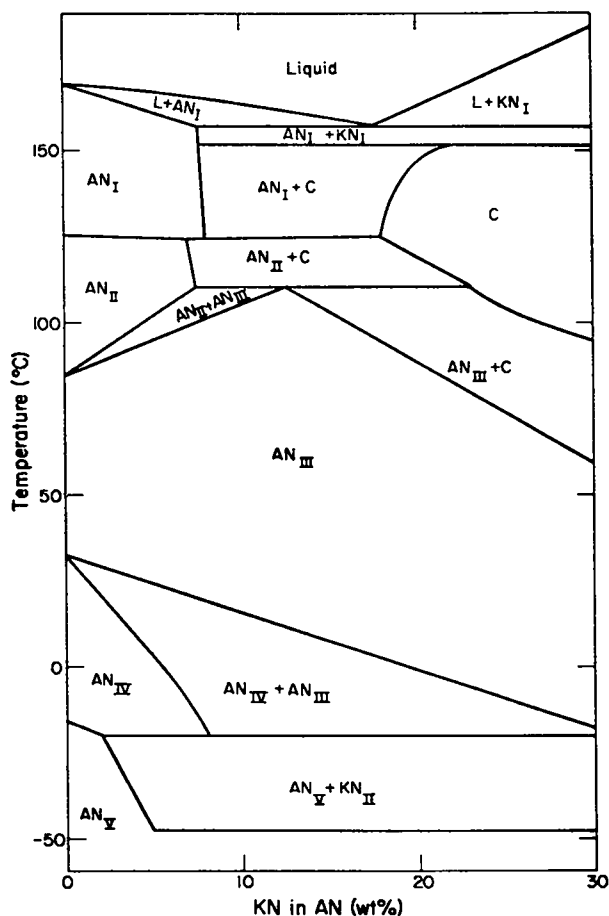


Fig. 7. AN-KN phase diagram reported by Jänecke et al.<sup>8</sup>



Several Russians reported<sup>9</sup> the phase diagram given in Fig. 8. This phase study did not extend into the region below room temperature; and our agreement with their results is not good, but they did report the high temperature phase, C I.

Coates and Woodard<sup>10</sup> published an x-ray diffraction determination of the AN-KN phase diagram and their results are shown in Fig. 9. The differences between this phase diagram and ours are substantial but perhaps the most significant is the interpretation of the C II phase as KN III. Figure 9 also shows the AN III-AN IV phase transition line determined by Campbell and Campbell<sup>11</sup> which is in exact agreement with ours.

Figure 10 shows the phase diagram reported by Morand.<sup>12</sup> This diagram was estimated from DTA curves and does not agree with our results.

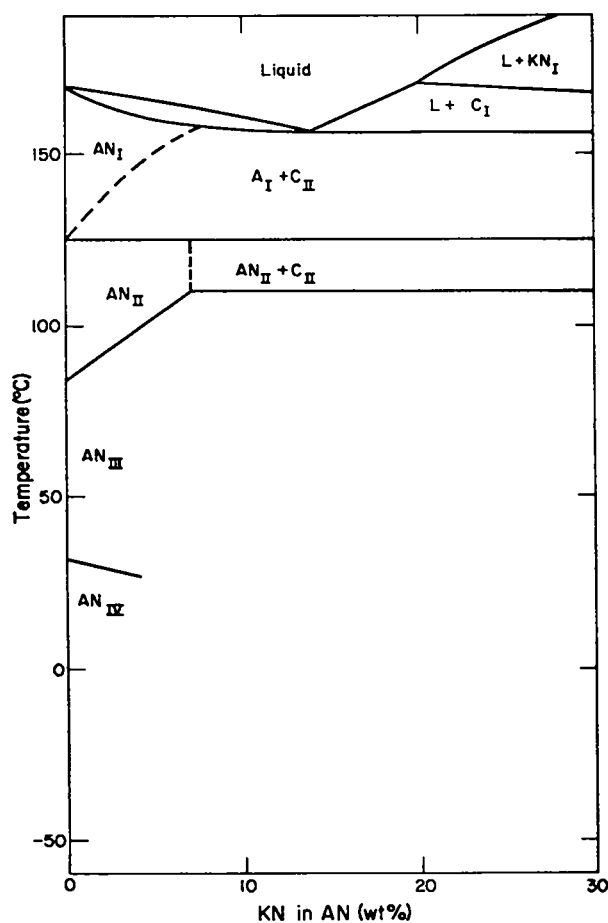


Fig. 8. AN-KN phase diagram reported by Bergman et al.<sup>9</sup>

(5) Discussion. The phase diagram (Fig. 6) shows that there is no KN concentration that stabilizes AN III over the entire temperature range of military interest. Addition of about 15% KN to AN before prilling is still a likely technique for dimensionally stabilizing Amatex. There are three reasons that this technique should work. First, the AN III to AN V and AN III to AN IV transformations are very slow, particularly for dry AN. Secondly, there is almost no density change on converting from AN III to AN V. Finally, the AN IV phase is never stable and AN III will probably never undergo the large volume change transformation to the AN IV polymorph.

The hypothesis that Amatex can be stabilized by KN should be checked experimentally by

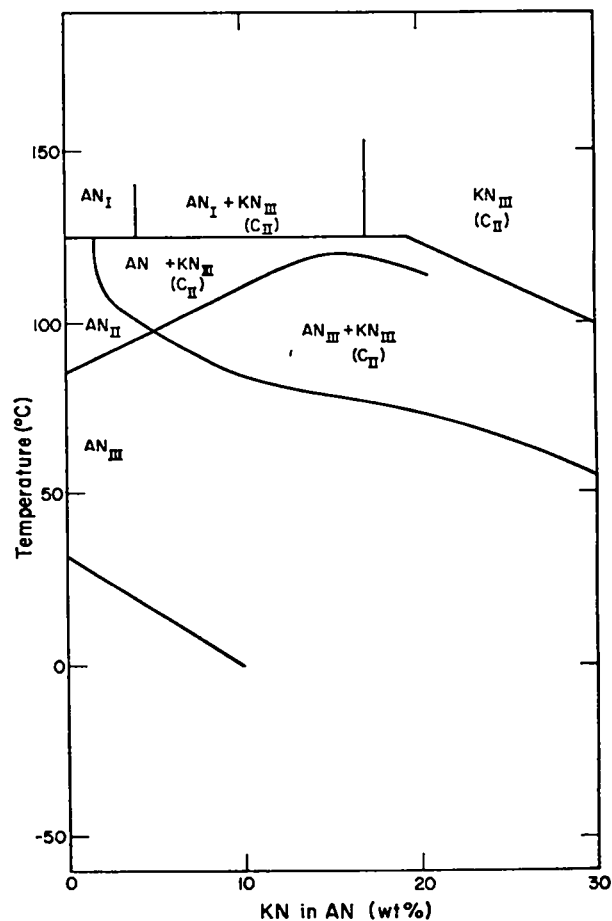


Fig. 9. AN-KN phase diagram reported by Coates and Woodard,<sup>10</sup> and Campbell and Campbell.<sup>11</sup>

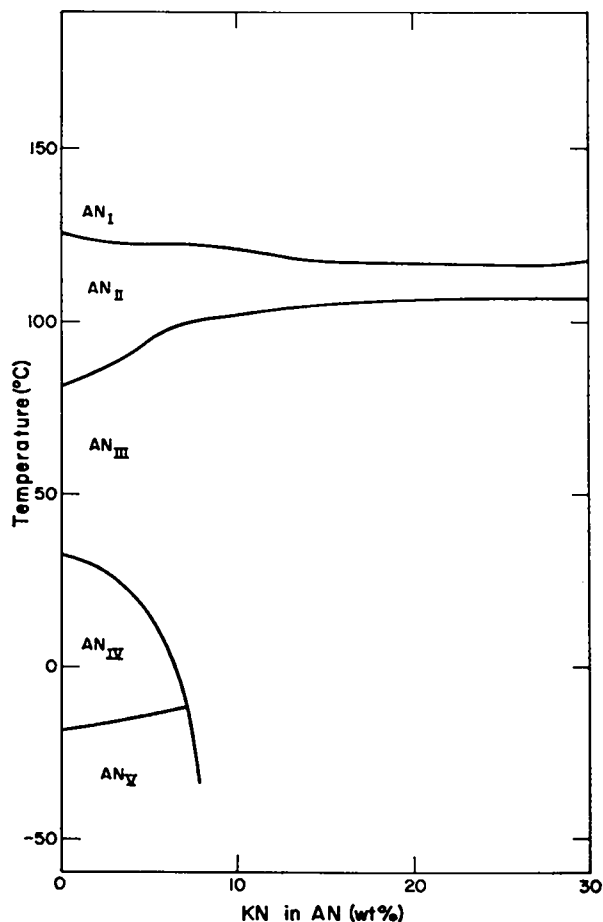


Fig. 10. AN-KN phase diagram reported by Morand.<sup>12</sup>

simulating arctic storage conditions. We recommend that the AN prills tested should have 10, 15, and 20 wt% KN added, that some charges be prepared with AN prills that have been dampened with an ethylene glycol water solution, and that the cycle time be adjusted so that the charges are below  $-15^{\circ}\text{C}$  for more than a week on each cycle. No phase change will occur in the AN III while casting the charges.

### 3. Future Work

Work on the processing characteristics of Amatex formulations will be continued with emphasis on the use of NC as a surface active compound. The optimum concentration of NC will be determined. The relative energy of Amatex formulation as a function of AN particle size (including prills)

will be determined. Preliminary studies of the initiability of Amatex should be completed and provide the information required to perform more quantitative experiments.

## B. ANALYSIS OF PREMATURES (TASK B), C. A. Anderson, C. L. Mader, B. G. Craig

### 1. Introduction

Prematures are usually associated with defects in the fuse, the projectile case, or the explosive fill. Typical of the first two defects is a faulty fuse leading to premature initiation or a faulty base plate closure that leads to ignition of the explosive by the hot propellant gases. Defects in the explosive fill itself are, to date, the least understood of the three causes, and therefore, are the subject of this investigation. The puzzling aspects of prematures caused by explosive defects have resulted in the comprehensive proof testing of gun/shell components, and the development of experimental premature simulators.

The accidental initiation of high explosives has been the subject of study for many years. Calculational models that rely on heating caused by shock compression of the explosive have been formulated and have been found applicable over a wide range of initiation phenomena. In general, shock pressures in the range of tens to hundreds of kilobars are required to initiate detonation in solid explosives, and the initiation times are in the order of microseconds. Even so, some investigators feel that a low amplitude shock, at the kilobar level, can be built up to an initiating level by the method of shock interactions.

The main purpose of this investigation will be to study the potential for thermal ignition produced in situations of confinement and relatively low stressing of high explosives, typical of those that exist during a projectile launching. The ultimate goal will be to identify critical explosive and loading parameters, and to correlate calculational models with data collected in controlled experiments and observed in large caliber gun prematures.

## 2. Progress This Report Period

### a. Theoretical

The one-dimensional reactive hydrodynamic code SIN<sup>13</sup> was used to obtain a numerical description of the underwater premature experiments of Craig described in the previous progress report.<sup>4</sup>

The numerical model consisted of a 12.7-mm-radius sphere of PBX 9404 explosive containing a 1.587-mm PETN initiator at the center surrounded by a 4.7628-mm-thick shell of PETN. The explosive sphere was surrounded by 96.8 mm of water, 1.5 mm of Plexiglas, 1.0 mm of air, 25.4 mm of TNT, and finally 60 mm of water. A calculation was also performed with a model that eliminated the air.

The equations of state for the PETN, PBX 9404, and water were identical to those used for the underwater detonation calculations described in Refs. 14 and 15. The air was described using the isentrope for air calculated with the BKW equation of state<sup>16</sup> and with an ideal gas equation of state. The TNT and Plexiglas equations of state were determined using the experimentally measured single shock Hugoniot and the Grüneisen equation of state. For Plexiglas, the Hugoniot is described by  $U_s = 0.243 + 1.5785 U_p$  (where  $U_s$  is shock velocity and  $U_p$  is particle velocity),  $\rho_0 = 1.18 \text{ Mg/m}^3$ , and  $\gamma = 1.0$ . For TNT, the Hugoniot is described by  $U_s = 0.3033 + 1.366 U_p$ ,  $\rho_0 = 1.624$ ,  $\gamma = 1.73$ .

The SIN code also includes the effect of heat conduction. While it is possible to run the calculations with both hydrodynamic and conductive transfer of energy, it is more economical to perform two separate calculations with the hydrodynamic state values at maximum compression being used as the starting conditions for the heat conduction and reaction calculation.

The heat conductivity constants used for Plexiglas and TNT were 0.157 and 0.259 MPa/m<sup>3</sup>/K/m/ $\mu$ s, respectively. The air heat conductivity constant was described by 0.026 [Temperature (K)/300<sup>0.5</sup>].

The SIN code gives nearly identical results to those described in the previous progress report<sup>4</sup> for problems of heat transfer across air gaps.

The reaction kinetics were described using the Arrhenius rate law and the Zinn and Rogers<sup>17</sup> parameters of 173 kJ/mol for activation energy and  $1 \times 10^7 \mu\text{s}^{-1}$  for frequency factor.

The calculation without air between the Plexiglas and TNT gave a maximum TNT shock pressure of 370 MPa and a temperature rise of approximately 5 K. It is not surprising that no reaction was experimentally observed for the system without an air gap. The pressure at the TNT-Plexiglas interface had decreased to 180 MPa by the time the shock wave had traveled through the TNT explosive. The front of the shock wave was 250 MPa upon arrival at the TNT-water interface. The time for the shock to travel through the TNT was about 8  $\mu$ s. The calculated water shock pressure upon arrival of the shock at the Plexiglas-water interface was 200 MPa, approximately linearly decreasing to 100 MPa at 20 mm behind the Plexiglas-water interface.

In the calculation with 1 mm of air, the gap took 6.5  $\mu$ s to close. The maximum air pressure was 340 MPa, density 0.41 Mg/m<sup>3</sup>, particle velocity 0.0675 mm/ $\mu$ s, and the gap was compressed to 1/320 of its original thickness, or 0.0031 mm. The maximum temperature of the gas was 2700 K.

Using these results as the starting conditions for the heat transfer calculation gave a maximum temperature of 820 K in the TNT and 910 K in the Plexiglas. The temperature in the gas was lowered to a maximum of 2000 K within 3  $\mu$ s and insufficient reaction had occurred for the first cell to decompose. At later times the explosive surface cooled as heat was being conducted away faster than furnished by the hot gas and the explosive decomposition.

The conclusions are not sensitive to the gas temperature calculated, as the initial compressed

gas temperature could be more than 1000 K higher than calculated and still be insufficient to result in any appreciable decomposition at the TNT surface.

Since the calculation does not include the effects of side rarefactions on the Plexiglas-air-TNT cylinder, these results must be considered upper limit values.

Identical calculations with the air described by an ideal gas equation of state with a  $\gamma$  of 1.28 and  $C_v$  of 1.04 KJ/kg/K gave a maximum air pressure of 354 MPa, density of 0.76 Mg/m<sup>3</sup>, particle velocity of 0.07 mm/ $\mu$ s, and maximum gas temperature of 1900 K. The gas temperature using the ideal gas air equation of state is about 800 K lower than calculated using the more realistic BKW air equation of state.

The experimental observations were that approximately the same amount of decomposition was observed for 1.0 mm of air, krypton, methane, or vacuum. Our most favorable calculations indicate that heat conduction alone is insufficient for appreciable reaction to occur for air gaps of this thickness or a vacuum and that the methane-filled gap should give TNT temperatures at least 300 K lower than the krypton-filled gap. Therefore, we apparently have established that some phenomenon other than plane surface heat conduction is dominating the initiation process of the explosive in the aquarium experiment. Some mechanism is required for the heat in the gas to be concentrated in local areas of the explosive surface or some other source of initiation energy is required such as shock interactions or internal void compression. The concentration mechanism appears to be relatively independent of the gas temperature and perhaps entirely independent of the kind of gas.

#### b. Experimental

An aquarium technique for studying the effect of base gap, surface finish, and surface coating was described in the previous report.<sup>4</sup> Several experiments were described and photographs of recovered samples of pressed TNT,  $\rho_0 = 1.611$

Mg/m<sup>3</sup>, were given. In one experiment, two samples of TNT were confined in steel but did not detonate. A photograph of the steel chambers was shown but visual observations of the TNT adjacent to the base gap to determine if ignition occurred and was then extinguished were not made at the time the report was written.

The exposed surface of the TNT in the steel confined experiments is shown in Fig. 11. There is no evidence of ignition in the central region of either surface. Both samples were chipped near their perimeters; the sample exposed to a 5-mm-thick gap also was cracked near the center. The sample exposed to a 1-mm-thick gap had very minor discoloration at three of the larger chips around its perimeter; this phenomenon is believed to be due to edge effects. The Plexiglas disk used



Fig. 11. Surfaces of recovered samples of TNT confined in steel. The sample on the left had a base gap separation of 1 mm, that on the right had a separation of 5 mm. Other experimental details were given in the previous report.<sup>4</sup> The three larger chipped areas, which showed slight discoloration, are in the lower left portion of the sample on the left. The white around the perimeter of the sample on the right is due to the TNT being powdered in that region. The Plexiglas disks are below the sample they were used with.

to close the 5-mm-thick gap was broken along radii; the disk used to close the 1-mm-thick gap was cracked, but not broken, in a circular pattern.

The pressure was inadequate to heat the air in the base gaps sufficiently to ignite the explosive. The pressure was lower in these two experiments than it was in any of those described in the previous report (ca. 170 vs 290 MPa). This was because of the shock impedance mismatch between water-steel-air.

As noted in the previous report, polishing the pressed TNT revealed numerous small cavities. A tentative explanation for the apparent absence of effects due to surface finish or gas type was the dominance of the small cavities as an ignition source.

During the past quarter, TNT samples prepared in a variety of ways have been polished in an effort to determine what method of sample preparation results in surfaces free of such defects. A method has apparently been found and charges are being prepared for additional aquarium-type experiments. The object is not to prepare an insensitive TNT charge (although such may prove to be the case), but rather to prepare a charge that will allow us to determine the relative importance of a variety of variables.

### 3. Future Work

Additional aquarium tests will be performed with explosives having defect free surfaces. Polishing techniques are being developed in an effort to prepare these surfaces. Other initiation models, utilizing internal surface defects, and methods of concentrating energy in the defects will be tried to determine if sufficient thermal energy is generated to initiate ignition.

### C. SYNTHESIS OF HMX (TASK C)

Funds allocated for this task were expended during the first two quarters and results were reported in the reports previously issued.

Additional work is being conducted with funds provided by PA.

### D. INITIATION AND SENSITIVITY (TASK D), B. G. Craig

#### 1. Introduction

The ultimate objective of this investigation is to obtain a quantitative understanding of the mechanisms leading to the initiation of a violent reaction in the high explosive. One approach to developing a quantitative model of the initiation is to study the response of an explosive subjected to a single shock of known amplitude and duration in a one-dimensional system. This requires the development of a plane wave shock generator and supporting instrumentation for use in experiments to generate data that can be used to define the state of the shocked explosive as a function of time and initial conditions.

#### 2. Progress This Report Period

Considerable difficulties have been encountered in the design of a flyer plate, plane wave shock generator. A study of the quantitative response of explosives cannot be started until these problems have been resolved.

#### 3. Future Work

Work will continue on the design of plane wave generators and the instrumentation required to measure the amplitude and duration of the shock pulse.

#### REFERENCES

1. A. Popolato, A. W. Campbell, L. W. Hantel, H. R. Lewis, P. G. Salgado, and B. G. Craig, "Properties of Amatex/20," Los Alamos Scientific Laboratory report LA-5516-MS (March 1974).
2. J. R. Van Waser, J. W. Lyons, K. Y. Kim, and R. E. Colwell, Viscosity and Flow Measurements (Interscience Publishers, Inc., New York, 1963), Chap. 3, pp. 150-155.

3. H. Green, Industrial Rheology and Rheological Structures (John Wiley and Sons, Inc., New York, 1944), pp. 38-40.
4. A. Popolato, "Joint Services Explosive Program," Los Alamos Scientific Laboratory report LA-5521-PR (March 1974).
5. C. Boyars, J. R. Holden, and A. L. Bertram, "Minol IV, A New Explosive Composition Containing Ammonium Nitrate-Potassium Nitrate-Solid Solution: Part I," Naval Ordnance Laboratory report NOLTR-73-49 (1973).
6. R. N. Brown and A. C. McLaren, "On the Mechanism of the Thermal Transformations in Solid Ammonium Nitrate," Proc. Royal Soc. A266, 329-343 (1962).
7. W. C. McCrone, Fusion Methods in Chemical Microscopy (Interscience Publishers, Inc., New York, 1957).
8. E. Jänecke, H. Hamacher, and E. Rahlfs, "The System  $\text{KNO}_3$ - $\text{NH}_4\text{NO}_3$ - $\text{H}_2\text{O}$ ," Z. Anorg. Allgem. Chem. 206, 357-368 (1932).
9. A. G. Bergman, V. P. Radishchev, I. N. Nikonova, V. N. Sveshnikova, E. B. Shternina, and M. A. Yatsuk, "External Components in the Fusion Diagram of the Quarternary Reciprocal System  $\text{NH}_4$ ,  $\text{K} \mid \text{Cl}$ ,  $\text{NO}_3$ ,  $\text{H}_2\text{PO}_4$ ," Izvest. Sekora Fiz. Khim. Anal. Obshch. Neorg. Khim. Akad. Nauk SSR 15, 157-199 (1947).
10. R. V. Coates and G. D. Woodard, "An X-ray Diffractometric Study of the Ammonium Nitrate-Potassium Nitrate System," J. Chem. Soc. 1965, 2135-2140 (1965).
11. A. N. Campbell and A. J. R. Campbell, "The Effect of a Foreign Substance on the Transition:  $\text{NH}_4\text{NO}_3$  IV  $\rightleftharpoons$   $\text{NH}_4\text{NO}_3$  III," Can. J. Res. 24B, 93-108 (1946).
12. J. Morand, "A Study of Ammonium Nitrate and its Solid Solutions," Ann. Chim. 10, 1018-1060 (1955).
13. C. L. Mader, "FORTRAN SIN - A One-Dimensional Hydrodynamic Code for Problems Which Include Chemical Reaction, Elastic-Plastic Flow, Spalling and Phase Transitions," Los Alamos Scientific Laboratory report LA-3720 (1967).
14. C. L. Mader, "Compressible Numerical Calculations of Underwater Detonations," Los Alamos Scientific Laboratory report LA-4594 (1971).
15. C. L. Mader, "Detonations Near the Water Surface," Los Alamos Scientific Laboratory report LA-4958 (1972).
16. C. L. Mader, "FORTRAN BKW - A Code for Computing the Detonation Properties of Explosives," Los Alamos Scientific Laboratory report LA-3704 (1967).
17. J. Zinn and R. N. Rogers, "Thermal Initiation of Explosives." J. Phys. Chem. 66, 2646 (1962).

DISTRIBUTION	<u>No. of Copies</u>
Director ARPA, Attn: Program Management, Arlington, VA 22209	3
Dr. Charles Ravitsky, ARPA, Arlington, VA 22209	1
Dr. Ray Thorkildsen, DDR&E, The Pentagon, Washington, D. C. 20301	1
F. E. Walker, LLL, Livermore, CA 94550	2
R. F. Walker (SMUPA-FR-E), Picatinny Arsenal, Dover, NJ 07801	2
L. W. Saffian (SMUPA-MT), Picatinny Arsenal, Dover, NJ 07801	1
D. E. Seeger, Explosives Application Section, Picatinny Arsenal, Dover, NJ 07801	1
Maj. Gen. Ernest Graves/D. I. Gale, DMA, USAEC, Washington, D. C. 20545	1
H. J. Gryting, NWC, China Lake, CA 93555	1
A. B. Amster, NOSC, Washington, D. C. 20360	1
J. E. Ablard, NOL, Silver Spring, MD 20910	1
D. Price, NOL, Silver Spring, MD 20910	1
M. Kamlet, NOL, Silver Spring, MD 20910	1
C. Boyars, NOL, Silver Spring, MD 20910	1
M. F. Zimmer, AFATL/DLIW, Eglin AFB, FL 32542	1
D. K. Nowlin/M. D. Roepke, USAEC ALO, Albuquerque, NM 87115	1
Capt. R. R. McGuire, FJSRL, USAF Academy, Colorado Springs, CO 80840	1
P. M. Howe (AMXRD-OD), BRL, APG, Aberdeen, MD 21005	1
 INTERNAL LASL DISTRIBUTION	
D. P. MacDougall	1
A. D. McGuire	1
E. H. Eyster	1
M. L. Brooks	1
W. E. Deal	1
J. R. Travis/B. G. Craig/A. W. Campbell	3
P. A. Carruthers/C. L. Mader	1
L. C. Smith/M. D. Coburn/H. H. Cady/T. M. Benziger	4
J. Aragon	1
A. Popolato	1
C. A. Anderson	1
T. Rivera	1